REVISTA MATÉRIA V.30
ISSN 1517-7076 articles e20250255, 2025

Comparison of thermal conductivity measurement methods for reprocessed EVA material sheets

Balakrishnan Krishnan[1], Dhavamani Chinnathambi[1]

[1]Mahendra Engineering College, Department of Aeronautical Engineering. 637503, Namakkal, Tamilnadu, India.
e-mail: kbaluaero@gmail.com, dhava.cs@gmail.com

ABSTRACT

This study aims to analyze and compare two methods for measuring the thermal conductivity of EVA sheets obtained from reprocessed industrial scraps. The experiments were conducted using a cylindrical wall method and a flat plate propagation method to evaluate their cost-effectiveness, accuracy, and compliance with current standards. Results indicate that the cylindrical wall method is more cost-efficient (($0.042) compared to the flat plate method (($1.25). However, the flat plate method better simulates real conditions by providing the necessary time for thermal equilibrium. The lowest thermal conductivity was observed in the thin blanket (TNB) configuration (0.66 W/m°C), whereas the highest conductivity was noted in the configuration with two thick blankets (2TKB) (42.4 W/m°C). Both methods showed consistency with existing standards, with further calibration required using standard insulation materials. These findings suggest that the tested Ethylene Vinyl Acetate sheets (EVA) sheets are viable thermal insulators with satisfactory attenuation properties.

Keywords: EVA Sheets; Thermal Conductivity; Thermal Insulation; Cylindrical Wall Method; Flat Plate Method.

1. INTRODUCTION

Ethylene Vinyl Acetate (EVA) is a versatile polymer known for its unique combination of flexibility, toughness, and lightweight properties [1]. Comprising ethylene and vinyl acetate copolymers, EVA exhibits characteristics such as high elasticity, resistance to stress cracking, and excellent shock absorption [2]. These properties have made EVA widely popular in various industries, including footwear, packaging, insulation, and cushioning. One of the significant applications of EVA sheets is in the production of footwear components, such as midsoles and insoles, due to their lightweight and cushioning properties [3].

In recent years, the importance of thermal insulation has grown in numerous engineering fields, from construction to electronics, due to the increasing demand for energy efficiency and thermal management [4]. Thermal conductivity is a crucial thermophysical property that defines a material's ability to transmit heat. Materials with low thermal conductivity are classified as thermal insulators, whereas those with high conductivity are considered thermal conductors. Selecting suitable thermal insulation materials is vital for applications such as building insulation, protective clothing, and electronic devices [5].

The footwear industry generates a significant amount of EVA scrap during the manufacturing process. Traditionally, these scraps are disposed of as waste, contributing to environmental pollution. However, due to the thermoplastic nature of EVA, these scraps can be reprocessed and recycled into new sheets, providing an eco-friendly and cost-effective material source. In India, where the footwear industry is one of the largest in the world, effective recycling and reuse of EVA scraps can contribute to sustainability and circular economy practices. The growing focus on sustainability has motivated researchers to explore recycled materials for thermal insulation applications [6]. Reprocessed EVA sheets, made from industrial scraps, present an opportunity to develop cost-effective and efficient thermal insulators, especially in regions where thermal management is essential due to extreme weather conditions.

Measuring thermal conductivity is crucial for evaluating the insulation performance of materials. However, conventional methods often require expensive and sophisticated equipment, limiting their accessibility for small-scale industries and research facilities. There is a need for alternative, cost-effective methods to measure the thermal conductivity of recycled EVA sheets while ensuring accuracy and compliance with current standards [7].

Corresponding Author: Balakrishnan Krishnan Received on 19/03/2025 Accepted on 13/06/2025

DOI: https://doi.org/10.1590/1517-7076-RMAT-2025-0255

BÖRCSÖK and PÁSZTORY [8] conducted a comprehensive review on the role of lignin in woodworking processes involving elevated temperatures. Their study, published in the European Journal of Wood and Wood Products, emphasizes lignin's influence on the thermal stability and mechanical properties of wood. Lignin, a complex biopolymer, is crucial in enhancing wood's resistance to thermal degradation due to its aromatic structure. This property is particularly useful in high-temperature woodworking processes, such as thermal modification and hot-pressing. The study highlights that understanding lignin's behavior under heat is essential for optimizing manufacturing techniques and improving the durability and performance of wood products. Additionally, the authors note that lignin's thermoplastic nature can be leveraged to create wood composites with enhanced properties.

KALAMI *et al.* [9] explored the potential of using lignin as a substitute for phenol in phenolic adhesive formulations. Published in Industrial Crops and Products, this study investigates various types of lignin, including Kraft, organosolv, and lignosulfonate, to understand their adhesive properties compared to conventional phenol-formaldehyde resins. The findings reveal that lignin can partially replace phenol in adhesive formulations, resulting in cost-effective and eco-friendly alternatives. However, the degree of substitution and the performance of the adhesives depend on the source and chemical modification of the lignin. The study suggests further research on chemical modifications to enhance lignin's reactivity and bonding strength, thus making it a more viable alternative for industrial applications.

ELSHEIKH *et al.* [10] reviewed the advancements in wood-plastic composites (WPCs), focusing on pre-processing treatments, manufacturing techniques, recyclability, and environmental impact. Published in Cleaner Engineering and Technology, the study discusses the role of lignin as a reinforcing agent in WPCs. Lignin enhances the mechanical properties and thermal stability of composites while reducing production costs. Additionally, the study addresses challenges related to the compatibility between lignin and polymer matrices, emphasizing the need for surface treatments or compatibilizers. The review also highlights the importance of recycling and the eco-friendliness of lignin-based WPCs, aligning with the growing demand for sustainable materials.

LERMAN and SCHEEPERS [11] investigated the mass-transfer coefficient for wood drying using thermographic methods, as reported in Wood Material Science and Engineering. Their study presents an innovative approach to measuring moisture content and drying rates, utilizing infrared thermography to analyze the mass-transfer phenomena. The research shows that lignin's hydrophobic nature influences the drying rate, thereby affecting the overall mass-transfer coefficient. The findings contribute to the development of more efficient drying techniques, reducing energy consumption and improving the quality of dried wood products.

MISHRA *et al.* [12] reviewed the potential of converting lignin waste into value-added chemicals, contributing to the circular bioeconomy. Published in Science of the Total Environment, the study explores green chemical processes for lignin valorization, including catalytic depolymerization and bioconversion. The review highlights the potential of lignin-derived chemicals as sustainable alternatives to petroleum-based products, including phenols, vanillin, and biofuels. This approach supports waste minimization and promotes sustainable practices within the chemical industry, emphasizing lignin's role as a renewable feedstock.

FAVIER *et al.* [13] focused on enhancing the photodegradation efficiency of water pollutants using response surface methodology. Published in the Journal of Environmental Management, the study discusses the role of lignin-based photocatalysts in the degradation of organic pollutants. The incorporation of lignin into photocatalytic systems enhances light absorption and charge separation, improving the degradation efficiency of contaminants. This study highlights lignin's potential in environmental remediation and wastewater treatment, offering a sustainable solution to pollutant degradation.

NÄGELE *et al.* [14] introduced Arboform, a thermoplastic material made from lignin and natural fibers, as documented in Chemical Modification, Properties, and Usage of Lignin. Arboform exhibits thermoplastic behavior similar to conventional plastics but is biodegradable and derived from renewable resources. The material demonstrates excellent mechanical properties, thermal stability, and processability, making it a sustainable alternative to petroleum-based plastics. The study emphasizes the importance of lignin's aromatic structure in enhancing the strength and rigidity of Arboform, paving the way for its application in automotive components, consumer goods, and construction materials.

This study aims to evaluate two different methods for measuring the thermal conductivity of recycled EVA sheets sourced from industrial activities in the footwear sector. The two methods investigated are: the Cylindrical Wall Method, which utilizes a cartridge-type resistance to evaluate cylindrical propagation, and the Flat Plate Method, which measures thermal conductivity without considering the influence of convection and thermal radiation. The objectives of this study are to compare the efficiency and accuracy of the two methods, analyze the performance of the recycled EVA sheets as thermal insulators, evaluate the

Table 1: Summary of thermal conductivity evaluation methods for EVA.

METHOD	REFERENCES	MEASURES	ADVANTAGES	DISADVANTAGES
Hygrothermal Cycling	CONSTANTINO *et al.* [15]	Indirect thermal resilience	Simulates real-world environmental conditions; durability-focused	Does not provide quantitative thermal conductivity values
Transient Plane Source (TPS) / Laser Flash Analysis (LFA) / Differential Scanning Calorimetry (DSC) / Thermogravimetric Analysis (TGA)	KONG *et al.* [6], ELSHEIKH *et al.* [10], YE *et al.* [7]	Conductivity, stability, transitions	High accuracy; useful for detailed thermal and structural analysis	Requires expensive lab equipment; may be impractical for large-scale or in-situ testing
Infrared Thermography	LERMAN *et al.* [11]	Surface temperature, heat distribution	Non-contact, fast, suitable for surface inspection	Cannot assess through-thickness (bulk) conductivity; affected by surface emissivity
Cylindrical Wall & Flat Plate Methods (Proposed Method)	This Study	Bulk thermal conductivity (through-thickness); directional propagation	Cost-effective; adaptable for recycled EVA sheets; suitable for low-resource labs; simulates practical scenarios	Moderate precision compared to advanced methods; sensitive to setup consistency and material uniformity

cost-effectiveness of each method, and verify the adherence of the methods to current thermal conductivity measurement standards.

This study contributes to the growing body of research on recycled polymer materials by exploring the potential of reprocessed EVA sheets as thermal insulators. It provides a cost-effective approach to measuring thermal conductivity, which could be particularly beneficial for small-scale manufacturers and research facilities in developing countries like India. Additionally, the study supports the circular economy by promoting the reuse of industrial waste, aligning with sustainable development goals.

This research focuses on EVA sheets obtained from reprocessed scraps generated by the footwear industry. The study involves experimental analysis using two different thermal conductivity measurement methods, comparative evaluation of thermal performance, cost, and compliance with standards, and analysis of the effectiveness of EVA sheets as thermal insulators for potential applications in construction, packaging, and other relevant fields. By exploring cost-effective methods for measuring thermal conductivity and evaluating the potential of recycled EVA sheets as thermal insulators, this study aims to contribute to sustainable materials technology and promote environmental conservation.

Each method serves a distinct purpose in evaluating EVA's thermal performance. Thermal Conductivity Evaluation Methods for EVA is shown in Table 1.

2. MATERIALS AND METHODS

This section will describe the materials used to develop the tests performed, as well as the methods used to use each of them. The materials that were common in both tests are presented below.

• EVA sheets

The EVA sheets used as test specimens in the experiments were manufactured and supplied by Relaxo Footwears Ltd., a footwear company. These sheets are produced by reprocessing EVA scraps from the company's manufacturing process, where the scraps are ground and pressed to form the sheets.

Due to the difference in the composition of the materials used, the sheets used in the experiment are in two configurations, as explained below (Figure 1):

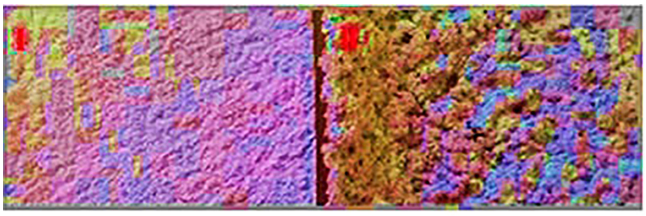

Figure 1: I. Thin sheet, II. Thick sheet.

The sheets were tested in six different configurations namely One thin sheet, One thick sheet, Two thin sheets, Two TKBs, One TNB (internal) and one TKB (external), One TKB (internal) and one TNB (external).

• Thermocouples

Three "K" type thermocouples were used to monitor the temperature in both tests, two of which were connected to two multimeters to monitor the temperature difference between the surfaces of the blanket, and a third thermocouple connected to the microcontroller.

This type of thermocouple is recommended for use in oxidizing and inert atmospheres up to 1372ºC. This means that it can be used at higher temperatures than other types of thermocouples.

2.1. Flat plate

To perform the experiment, a flat-wall apparatus was constructed to heat one side of the specimen while the other side was exposed to the environment and monitored for temperature. Figure 2 shows the basic construction of the apparatus [2].

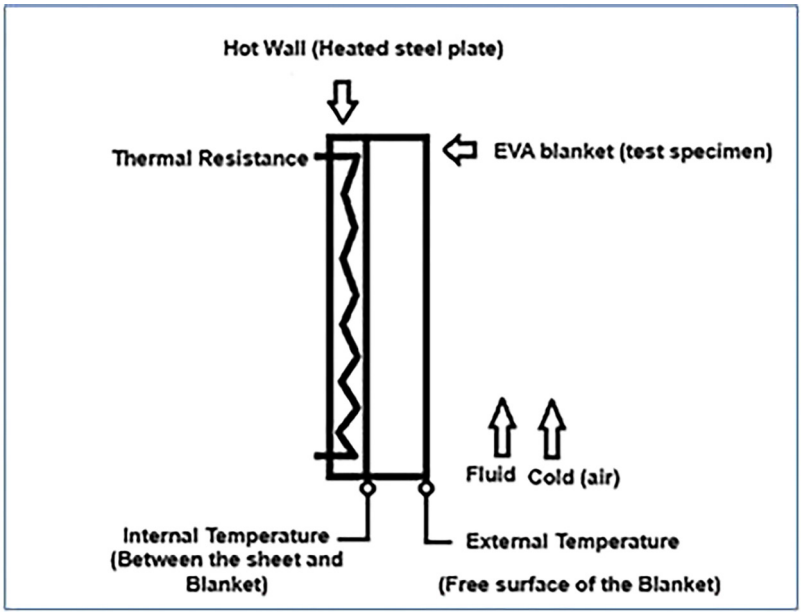

Figure 2: Basic structure of the apparatus.

The materials used to assemble this apparatus are as follows:

EVA sheets (test specimen): These were cut into pieces measuring 210 mm × 210 mm for attachment to the hot plate.

Hot plate: A 1020 steel plate measuring 300 mm × 300 mm × 12.7 mm was used as the hot plate and was fixed to a steel support.

Resistance: Heating was achieved using a spiral resistance fixed to the plate by eight ceramic beads, with temperature control managed by a microcontroller connected to the resistance.

Thermocouples: A system of three "K" type thermocouples was used to monitor the temperature. Two were connected to multimeters, and the third was connected to the microcontroller.

3. METHODS

The experiments to evaluate the thermal insulation capacity of EVA sheets were conducted based on the ISO 8302, ASTM C-177, ASTM C-518, and ASTM C-1114 standards, with some adaptations [2]. The method was applied by establishing an average temperature gradient across the EVA sheet through a steady-state heat flow, assuming one-dimensional conduction and free convection [2].

To set up the experiment, the 1020 steel plate was fixed to the steel support to ensure stability. Ceramic beads were then attached to one side, and the electrical resistance was installed, as shown in Figure 3.

Figure 3: Plate with beads and electrical resistance fixed.

Three thermocouples were installed to monitor the temperature. One was placed on the back of the plate, where the resistance was located, and was connected to the microcontroller to control the temperature increase. The other two thermocouples were connected to multimeters to monitor the temperatures within the blanket—one installed between the plate and the blanket (internal temperature) and the other on the free surface of the blanket (external temperature) [22].

Special care was taken to ensure flatness and maximum contact between surfaces, thereby enhancing heat transfer. The microcontroller started at 50°C, increasing by 50°C increments as the resistance stabilized at each point until reaching 200°C. However, due to the thermal resistance of the plate, the temperature at the face in contact with the blanket was lower. Measurements were recorded from the multimeter display every 5 minutes, and the test continued until no variation was observed between consecutive readings [2].

After collecting the voltage values from the multimeter, the voltage-to-temperature correlation table for the “K” type thermocouple was used to determine the internal and external temperatures at each point [2]. As the standardized thermocouple tables assume a reference junction at 0°C, whereas the experiments used ambient temperature as the reference, a correction factor of 0.8 mV (from thermocouple calibration) was added to each multimeter value before consulting the table [2].

Using the recorded temperatures, the efficiency at each point and the average efficiency of the configuration were calculated, allowing for an analysis of the most effective configuration [2].

3.1. Cylindrical wall [Cartridge Resistor]

Cartridge resistors are heating elements designed to operate over a wide range of temperatures while withstanding high thermal densities and mechanical impacts (Figure 4).

Their durability is due to a high-pressure manufacturing process and precision grinding. In this study, the cartridge resistor was used as a heating system because its cylindrical shape suited the project’s requirements, eliminating the need for additional assembly or test specimen modifications, which could have increased complexity and cost. The experimental setup for the cartridge resistor is shown in Figure 5.

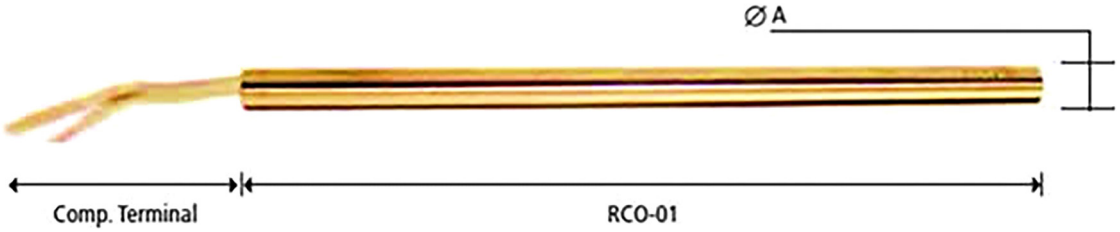

Figure 4: Cartridge resistor model.

Figure 5: Cartridge resistance assembly.

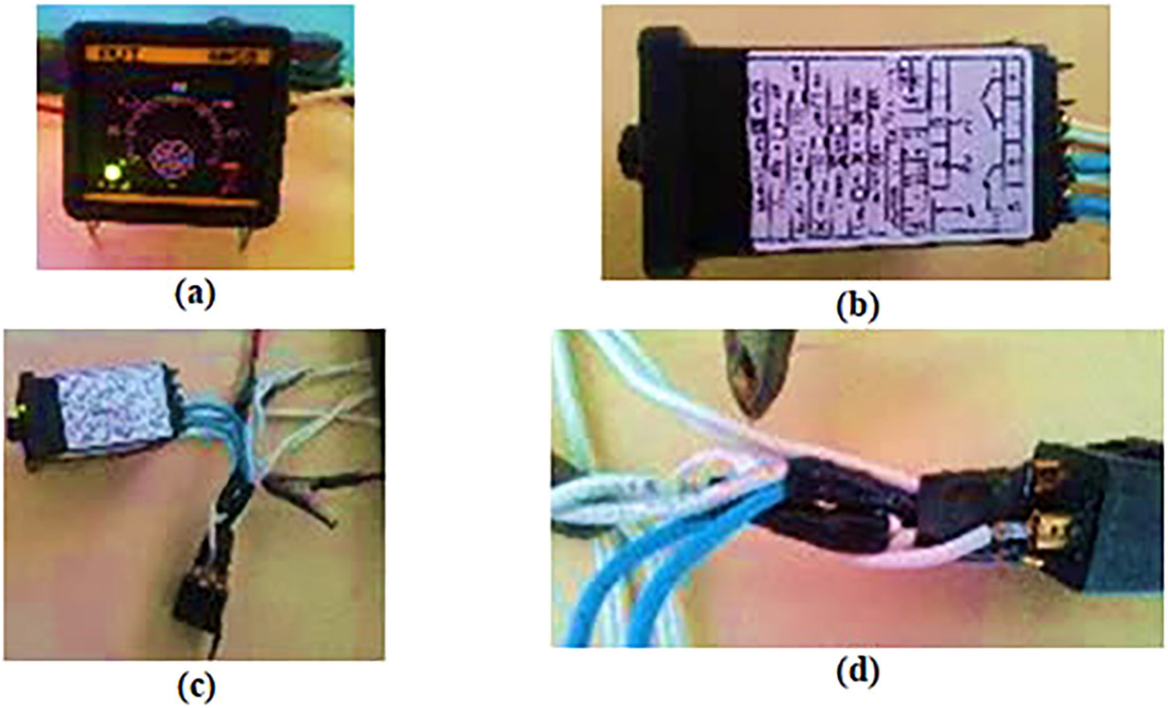

Figure 6: Temperature Control System. a) and b) controller and c) controller mounted on the relay and d) detailed assembly of the relay.

In this setup, a thermocouple in contact with the resistor controlled its temperature. The temperature control system is illustrated in Figure 6, which shows (a) and (b) the controller, (c) the controller mounted on the relay, and (d) the detailed relay assembly.

An external relay was necessary because the resistance's operating power required more current than the controller could provide, making the experiment otherwise unfeasible.

Figure 7: Test assembly.

The EVA compound served as the test specimen, functioning as the insulating material. Test specimens were arranged around the cartridge resistor to form cylindrical shells, ensuring complete thermal insulation at the ends, as depicted in Figure 7.

Different configurations were tested by varying insulation thicknesses and the number of layers to determine the most effective use of the material. Two configurations were tested:

- Single Wall: One layer of EVA covered the cartridge resistor. Tests were conducted using both the old and new composition blankets.
- Composite Wall: Two layers of EVA covered the resistor. Four tests were performed with this setup: the first with two layers of the old blanket, the second with two layers of the new blanket, and the last two with a combination of blankets. In the third test, the old composition blanket served as internal insulation with the new blanket externally, while this configuration was reversed in the fourth test.

Type K thermocouples, standardized by the American National Standards Institute (ANSI), were used due to their suitability for high-temperature environments—up to 1372°C. Composed of Chromel and Alumel alloys (Fig. 8), these thermocouples are widely used in industry due to their low cost and high tolerance.

Type	Composition
(+) Chromel	Ni (90%), Cr (10%)
(-) Alumel	Ni (95.4%), Mn (1.8%), Si (1.6%), Al (1.2%)

Figure 8: Composition of K-type thermocouple

During testing, the thermocouples were arranged in layers as follows:

- Thermocouples were pre-calibrated.
- One thermocouple was positioned at the interface between the cartridge heater and the test specimen to control the heater's temperature. It remained connected to the heater and controller throughout the tests.
- Another thermocouple was placed directly on the cartridge heater to measure its internal temperature.
- A third thermocouple was attached to the external region of the test specimen.
- All thermocouples were aligned at corresponding positions on both interfaces.
- Temperature readings were recorded in millivolts (mV) using multimeters. These readings were converted to °C using the K-type thermocouple table provided in the appendices.

Each test lasted between 7 and 8 minutes, depending on the heater's heating rate. Five measurements were taken for each temperature value, with data recorded whenever the controller switched on or off to maintain the set temperature. The materials and methods for the thermal efficiency analysis are illustrated in Figure 9.

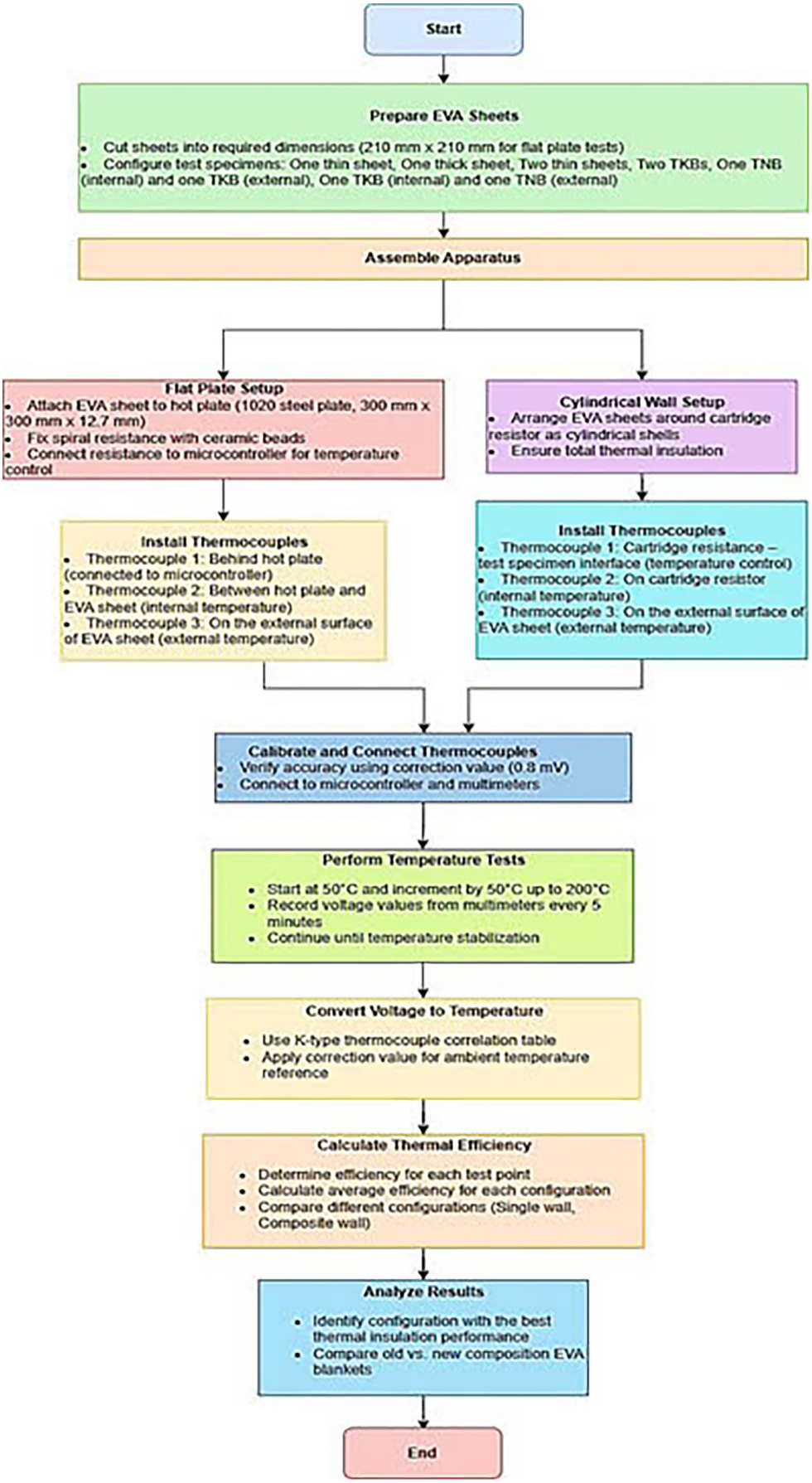

Figure 9: The materials and methods for the thermal efficiency analysis.

4. RESULTS AND DISCUSSIONS

The work flow of the thermal efficiency analysis is shown in Figure 10.

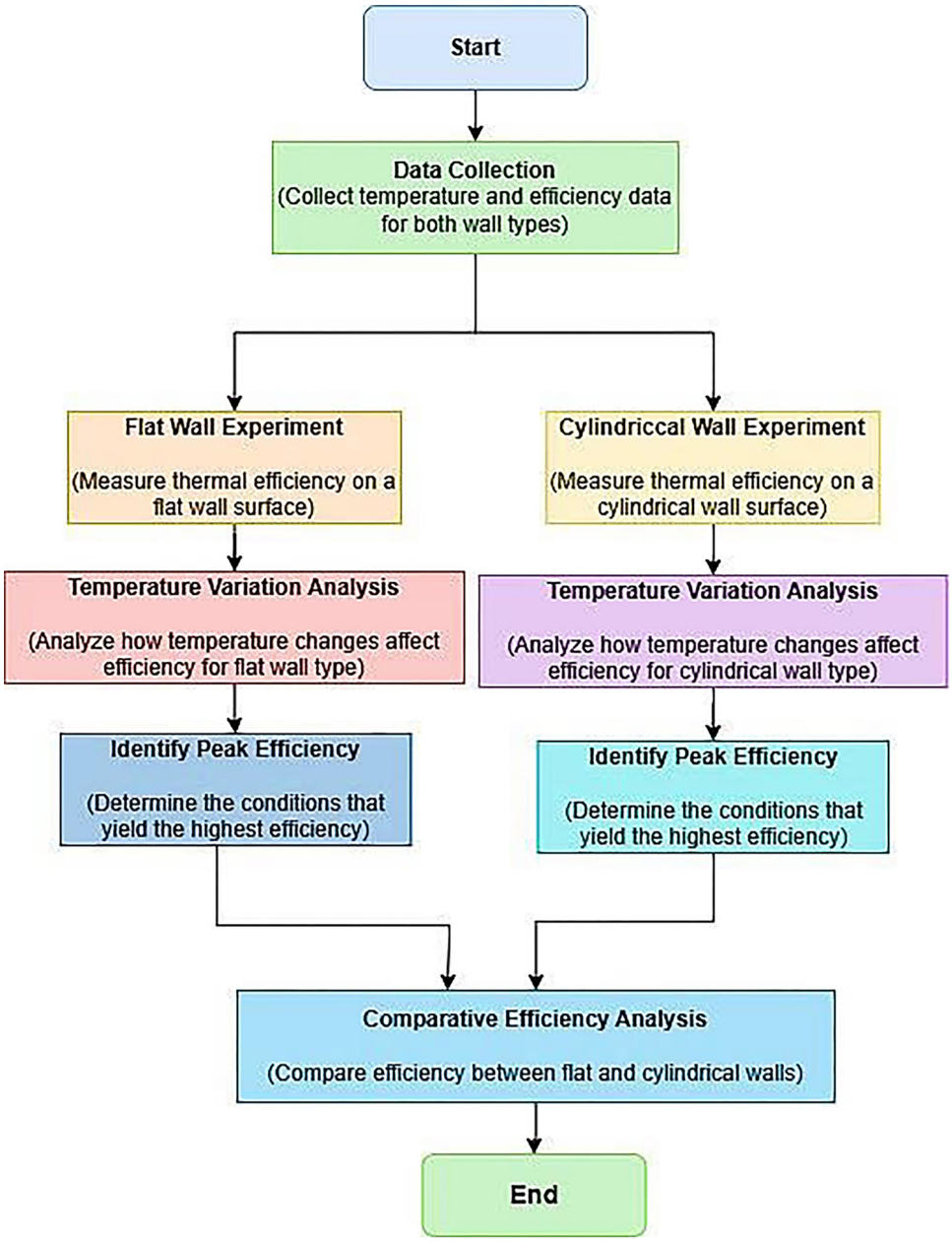

Figure 10: The work flow of the thermal efficiency analysis.

5. DATA PROCESSING

Below, we will see tables that illustrate the data collected and computationally processed after the tests were performed.

The data from the tests performed with the thin and TKBs will be treated qualitatively and quantitatively, comparing the flat and cylindrical methods of thermal analysis.

Through this data, it is possible to demonstrate the maximum temperature variation; the total test time, corresponding to the total energy consumed; as well as the comparison of the data on the efficiency of the blanket in attenuating heat for each test performed.

The table below (Table 2) illustrates the temperature variations, determined through the flat propagation experiment, for each configuration of the blankets and the time of the respective measurements.

Table 2: Temperature variation for each configuration – Flat wall.

FLAT PLATE: ΔT FOR RESPECTIVE ARRANGEMENT - ΔT [°C] AND TIME [MIN]											
1 THIN		1 THICK		2 THIN		2 THICK		THIN - THICK		THICK THIN	
TIME	ΔT	TIME	ΔT	TIME	ΔT	TIME	ΔT	TIME	ΔT	TIME	ΔT
5	17.4	5	22.1	5	9.9	5	22.1	5	17.2	5	29.7
15	31.4	15	43.5	20	38.7	15	53.5	15	41.3	15	53.4
25	33.8	30	58.0	30	50.6	30	79.8	30	62.8	30	79.8
35	33.8	40	67.9	45	62.9	40	89.6	40	77.4	45	96.9
45	41.3	50	73.0	75	68.4	55	99.7	50	89.9	60	107.4
55	39.0	60	78.1	85	66.1	70	110.0	65	100.0	75	110.2
60	39.1	75	85.6	100	61.3	90	90.9	80	105.2	85	107.9
65	39.1	80	85.6	105	61.3	95	90.9	85	105.2	90	107.9

According to the experiment carried out on the flat wall illustrated above, it is possible to conclude that the blankets present significant heat attenuation values, reaching a maximum attenuation point – data in red – and, after that, their efficiency is reduced.

Thus, it is observed that this fact occurred because the pores of the blankets opened at this maximum point of temperature variation, consequently the blankets began to release gases, causing the loss of heat and mass. After this point, the blankets reduced their insulation capacity, as they were soaked in heat.

It is worth noting that the experiment had a very long duration (ranging from 65 to 95 minutes), since the fixing of the resistance to the plate, through ceramic beads, caused a separation between them and caused the heat to be transmitted from the resistance to the plate by convection. In this way, the heat took a long time to reach the first surface of the blankets (in contact with the plate), since it had to soak the 8.9 kg plate that was in direct contact with the plate.

Below (Table 3) are presented and discussed the results for the cylindrical propagation experiment, which uses a cartridge-type resistor as a heat source.

It was possible to observe that there was no heat flow through the blanket up to a temperature of 100°C, since up to this temperature there was no variation in the temperature of the external surface of the blanket, which remained constant at a temperature of 20°C. A peak value was also not observed as in the flat wall experiment, since in this experiment the gases were only released when the configuration was disassembled when the blanket was removed from the resistor. With this, it was possible to reach the conclusion that the experiment did not last long enough to ensure that the blankets were soaked.

The insufficient time to ensure the blanket was soaked caused it to present greater heat attenuation, as there was not enough time for the heat to reach the outer edge of the blanket, leading to an illusory idea of good insulation.

Table 3: Temperature variation for each arrangement – Cylindrical Wall.

CARTRIDGE TYPE RESISTANCE: ΔT [°C] FOR RESPECTIVE ARRANGEMENT											
TN		TK		2TN		2TK		TN - TK		TK- TN	
SIZE	ΔT	SIZE	ΔT	SIZE	ΔT	SIZE	ΔT	SIZE	ΔT	SIZE	ΔT
1	18.7	1	12.3	1	17.7	1	12.3	1	13.8	1	19.2
2	45.6	2	30.9	2	36.7	2	27.9	2	31.8	2	48.7
3	64.7	3	54.0	3	59.3	3	49.7	3	56.4	3	77.6
4	96.1	4	79.0	4	88.8	4	82.0	4	79.1	4	114.7
5	113.9	5	102.3	5	118.1	5	110.7	5	103.4	5	161.5
6	117.7	6	130.1	6	123.6	6	141.5	6	135.5	6	190.0
7	127.1	7	159.4	7	149.6	7	174.5	7	167.1	7	225.2
8	133.6	8	189.1	8	192.8	8	215.8	8	198.1	8	263.5

Because they were in direct contact with the heat source – Resistance – the blankets presented some wear after the tests, some more than others, with the greatest wear occurring when the TKB was in direct contact with the resistance, leading to the conclusion that the TNB presents greater resistance to heat.

5.1. Comparative analysis of efficiency between the experimental methods

In order to compare the attenuation values for flat propagation and cylindrical propagation, a Table 4 was prepared with the efficiency results presented below, which is the average of the efficiencies calculated for each measurement of the temperature variation taken for the respective configuration of the blanket. The tabulated values of the average efficiency in heat attenuation are shown below.

Table 4: Average efficiency measurement of the blanket for each of the devices.

AVERAGE EFFICIENCY MEASUREMENT OF THE BLANKET FOR EACH OF THE APPLIANCES		
CONFIGURATION	FLAT PLATE η [AVERAGE]	CARTRIDGE RESISTANCE η [AVERAGE]
TNB	31.62%	53.4%
TKB	50.64%	70.2%
2 TNB	45.50%	74.9%
2 TKB	62.89%	75.0%
TNB-TKB	59.16%	74.4%
TKB-TNB	64.5%	79.4%

In both propagation methods, among the configurations of the blankets analyzed, those that stood out for presenting the greatest efficiency in insulation were the sixth configurations with an average efficiency of 64.5% for flat plate and 79.4% for cylindrical wall. The configuration that presented the lowest efficiency was the first one with the use of only one TNB, where for the flat and cylindrical wall an average efficiency of approximately 32% and 54% was obtained respectively.

Through these data it is possible to indicate that the TKB attenuates better when in contact with the hot source, and its effect is enhanced when it is externally coated by the TNB. When the reverse configuration (thin in direct contact with the resistance and thick on top) was tested, it showed a considerable drop in the efficiency of the set (from 79.4% to 74.4% on the cylindrical wall, and from 64.5% to 59.2% for the flat wall), even though it contained the same mass.

With these values, and in order to better visualize the comparison between the data, a Figure 11(a) was constructed illustrating the difference in efficiency for the same configurations differentiating the models of devices, as shown below.

Figure 11(b) shows a comparative analysis of the percentage efficiency of the two-wall geometry in different conditions (TN, TC, 2TN, 2TC, TN-TC, and TC-TN). In all cases, the efficiency of the cylindrical wall is several orders of magnitude higher than that of the flat wall. For example, in the TN condition, the efficiency of the cylindrical wall is 54%, while the efficiency of the flat wall is 32%, which is an improvement of 22%. In the 2TN condition, the efficiency of the cylindrical wall is the largest, reaching 75%, which is 30% higher than that of the flat wall. In all cases, the cylindrical wall maintains a high application value with low deformation and small errors. This consistent performance shows that the cylindrical wall geometry has a better operational advantage, which may be due to its better flow dynamics or thermal efficiency, which makes it more efficient in applications such as heat exchangers or fluid systems. In summary, this chart shows the advantages of using cylindrical walls to achieve high efficiency.

It can be seen in Figure 11(a) above that there is a certain parallelism between the curves, an average increase of 50% in the average efficiency values for the flat wall (red line), leading to an adhesion of the curves.

Therefore, it can be deduced that this 50% difference is due to some factors related to the assembly of the devices. For example, the loss of heat by convection on the flat wall, caused both by the distance between the resistance and the plate, and by the inadequate cutting of the blanket (small blanket did not cover the entire plate), leaving spaces on the surface, exposed to the action of convection, thus increasing the loss of heat through the edges. It should also be mentioned that the soaking time that did not occur on the cylindrical wall, which increased the attenuation values, thus not reflecting the real properties of the blankets.

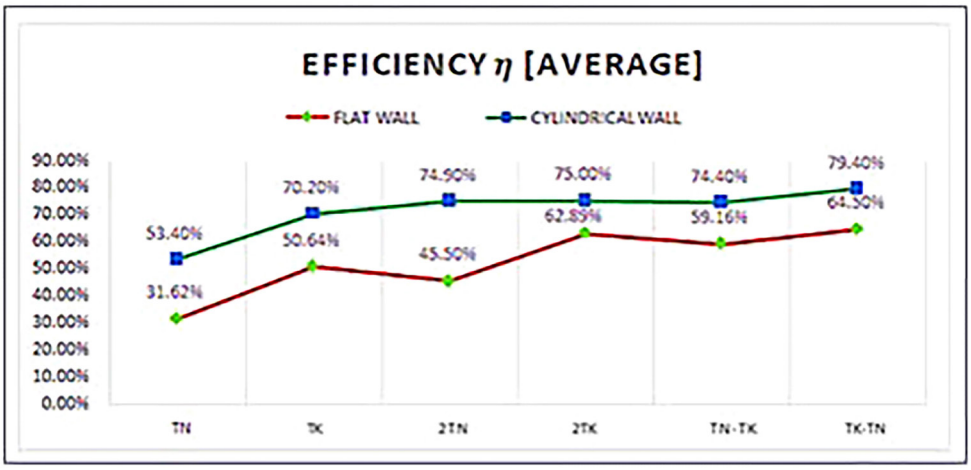

(a) Thermal efficiency of the blankets for each device

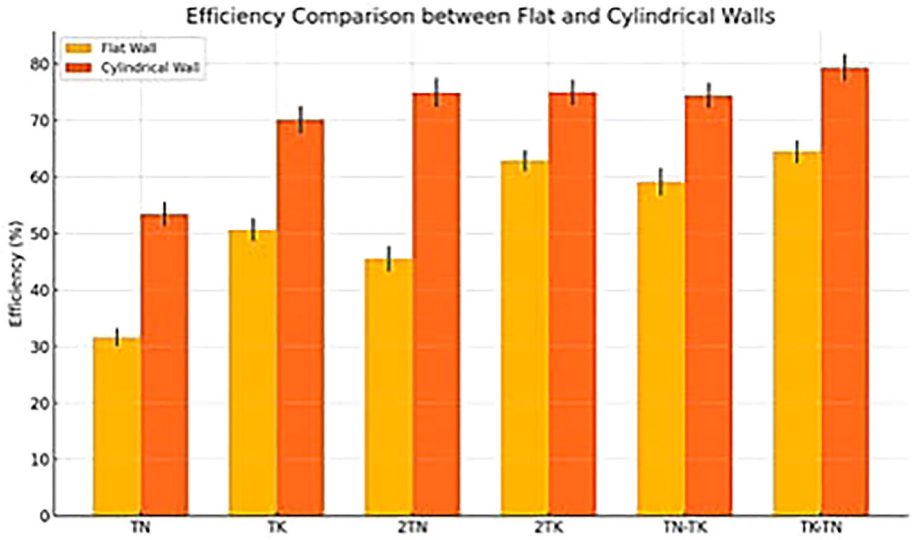

(b) Error Bars – Efficiency comparison between the two walls

Figure 11: Comparison of thermal efficiency of the blankets for each device.

According to the ASTM C 177 standard, the blanket must be cut in such a way as to cover the entire surface of the hot source, so that heat loss through the edges can be minimized and convective heating of the external thermocouple can be avoided from outside the blanket. It can be seen that the sample for the test on the flat wall was not cut in such a way as to cover the entire surface of the plate, not meeting this item of the standard, causing a considerable portion of heat to pass through convection through the edges to the external thermocouple.

5.2. Analysis of the consumption of the experimental methods

In order to quantify the energy consumption involved in the process, and thus be able to compare the energy efficiency of the use and application of the methods, data were collected from the spiral and cartridge resistances, as well as the time of each test, as shown below, Table 5.

Table 5: Cost and consumption data for each test.

CONSUMPTION AND COST						
TYPE	**POWER [W]**	**TIME [H]**	**POWER ([W])**	**TOTAL POWER [W]**	**COST (USD)**	**TOTAL COST [USD]**
Device	500.00	0.13	62.50	375.00	$0.008	$0.042

The individual times for each arrangement of the flat propagation are detailed, and lasted from 65 to 95 minutes. For the cylindrical propagation tests, the average time for each test was considered to be 7.5 minutes, since these lasted only 7 to 8 minutes. Five resets of the relay that powers the resistance were considered for each temperature tested, considering that these attempts to maintain the temperature would be sufficient for homogeneity, or a constant internal temperature.

The energy value was taken directly from the supplier's website, COELBA. The respective powers of each resistance are: 500 W for cartridge resistance and 1250 W for spiral resistance.

After performing the calculations, a large difference in energy consumption was noted. The flat wall method cost $ 1.21 in total and presented a consumption of around 29 times greater than the cylindrical wall method, which cost $ 0.04 for the 6 experiment configurations.

In order to illustrate the disparity between the methods' consumption, the Figure 12(a) is presented and discussed.

The data (Figure 12(b)) compares the heat capacity of flat walls and cylindrical walls at different conditions with their standard deviation (S.D.) and relative standard deviation (RSD%). In general, the effi-

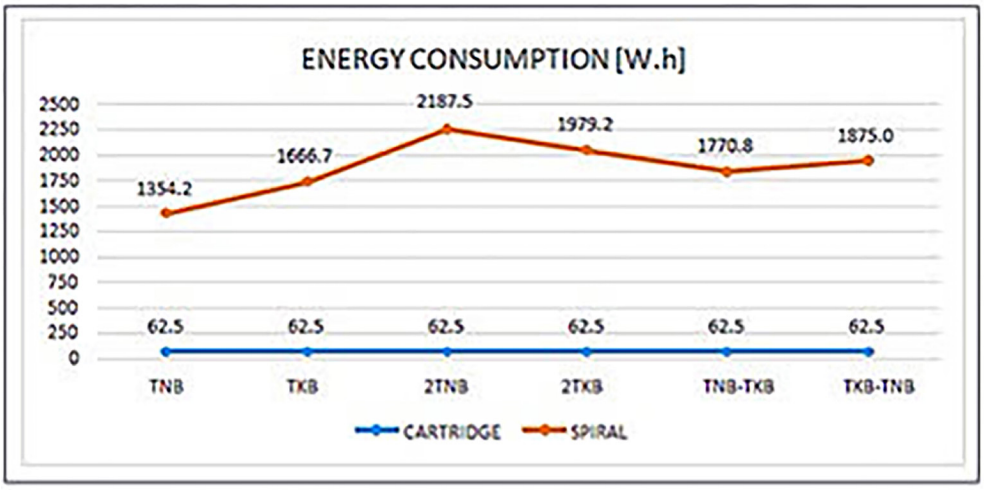

(a) Energy consumption of the apparatus

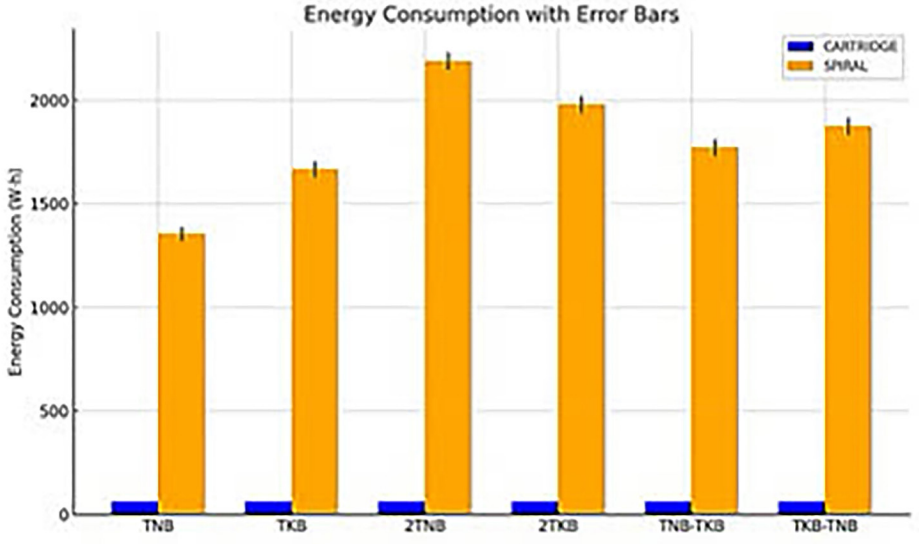

(b) Energy consumption with Error Bars

Figure 12: Energy consumption of the apparatus.

ciency of a cylindrical wall is always higher than that of a flat wall. For example, in the TN condition, the efficiency of the cylindrical wall reaches 53.40%, which is much higher than that of the flat wall of 31.62%. This pattern holds true in all cases, with the maximum efficiency achieved in the TK-TN case being 79.40% for the cylindrical wall and 64.50% for the flat wall. Both wall types show a general trend of increasing efficiency from simple heating cases (TN, TC) to complex or combined heating cases (2TC, TN-TC, and TC-TN), indicating that these configurations can improve the heat transfer efficiency. The variation of the measurements (expressed as S.D.) is small in all cases, indicating consistent results. This is further confirmed by the RSD values, which are typically in the range of 3% to 5%, which is acceptable for the experimental data. The percentage RSD for cylindrical walls (about 3-3.5%) is lower than that for planar walls (about 4-5%), indicating that cylindrical devices can provide more reliable and repeatable heating performance.

The observations in Figure 12(b) show a clear trend in power consumption between spiral and cartridge heaters. The power consumption of the spiral heater is consistently much higher than that of the cartridge heater under all experimental conditions. In particular, the power consumption of the spiral heater increases from the TNB case to the 2TNB case, peaks at around 2200 V•h, then decreases slightly in the 2TSB and TNB-TSB cases, and then increases again in the TCB-TNB case. In contrast, a cartridge heater has a low power consumption of 60 to 70 Wh with small fluctuations.

The error bars represent standard deviations, further highlighting the measurement differences. For cartridge heaters, the errors are very small, which indicates high measurement accuracy and low dispersion. For spiral heaters, when intermediate errors such as 2TNB and 2TSB occur, this leads to a large difference in energy consumption.

These findings indicate that although spiral heaters can generate more heat, their energy efficiency is significantly lower than cartridge heaters. The stability, low energy consumption, and low emissions of cartridge heaters are indicators of their reliability and performance. Therefore, if energy efficiency and stability are your priorities, cartridge heaters should be your first choice. Errors improve the reliability of the data, and the measurement control of cartridge heaters is more stringent.

The values for cylindrical propagation are presented as a straight line; the method has a relatively low consumption of 62.5 $W.h$ for each test, while the flat propagation method presents a high consumption, ranging from 1354.2 $W.h$ in the TNB, to 2187.5 $W.h$ in the double layer configuration of 2TNB. Among the methods analyzed, in terms of consumption and cost, the cylindrical wall test proved to be the most suitable, but the flat wall method, despite the losses due to convection, presented more reliable results because it is closer to real conditions.

5.3. Calculation of conductivity

To this end, only the cylindrical propagation method was used to obtain the values throughout the experiments, since it can only consider the conduction phenomenon, since convection in this case becomes negligible. The parameters for calculating the thermal conductivity of EVA sheets using the cylindrical propagation method include a cartridge-type resistance with a diameter of 22.5 mm and a length of 265.15 mm, resulting in a surface area of 0.01874235 m^2 for heat transfer. The resistance produces a power of 500 W, which is conducted through EVA blankets of two different thicknesses: 0.0033 m and 0.0098 m. These variations in thickness help assess their influence on thermal conductivity. By focusing solely on conduction and disregarding convection, this approach ensures accurate measurements of the thermal conductivity of the EVA sheets.

The conductivity was calculated using the equation adapted from the Fourier equation for cylindrical propagation,

$$k = \frac{qr \cdot ar}{2\pi rl\Delta T} \tag{1}$$

Where, q_r : Power of the cartridge type resistance, d_r: Thickness of the blanket, $2\pi rL$: Surface area of the resistance, The following Table 6 was then assembled with the respective values of the thermal conductivity of the EVA.

The values of the maximum and minimum temperature variations (maximum and minimum differences between the surfaces of the blanket) were selected to verify the minimum and maximum conductivities, respectively. The lowest conductivity value of 0.66 W/m°C (highest attenuation) was for the TNB when mounted alone in direct contact with the cartridge-type resistor.

The lowest conductivity (highest attenuation) was for the TNB of 0.66 W/m°C, while the highest conductivity (lowest attenuation) was for the configuration with two TKBs of 42.4 W/m°C. For insulating

Table 6: Conductivity measurements for maximum, average and minimum temperature variations.

	CONDUCTIVITY					
	TN	**TK**	**2TN**	**2TK**	**TN-TK**	**TK-TN**
MAXIMUM	4.69	21.24	9.89	42.38	25.29	18.26

materials, the expected conductivity value is 0 to 1 W/m°C, therefore only the single and double configurations of the TNB are within what is expected for an insulator.

According to the Argentine testing laboratory for materials, SAM – Asociación Argentina de Materiales testes – the thermal conductivity of EVA corresponds to 0.25 W/m °C. It is known that this value corresponds to virgin EVA, and that the blankets used in the tests are made by the company itself, Relaxo Footwears Ltd., therefore differing in their composition from that used by SAM, in addition to the varied density and degree of deformation for welding the particles.

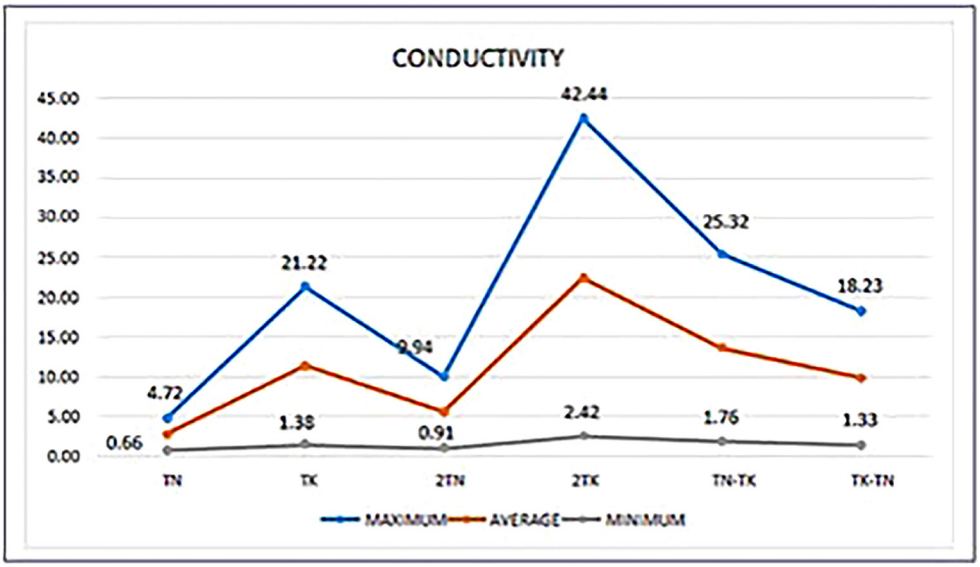

(a) Conductivity for due thickness

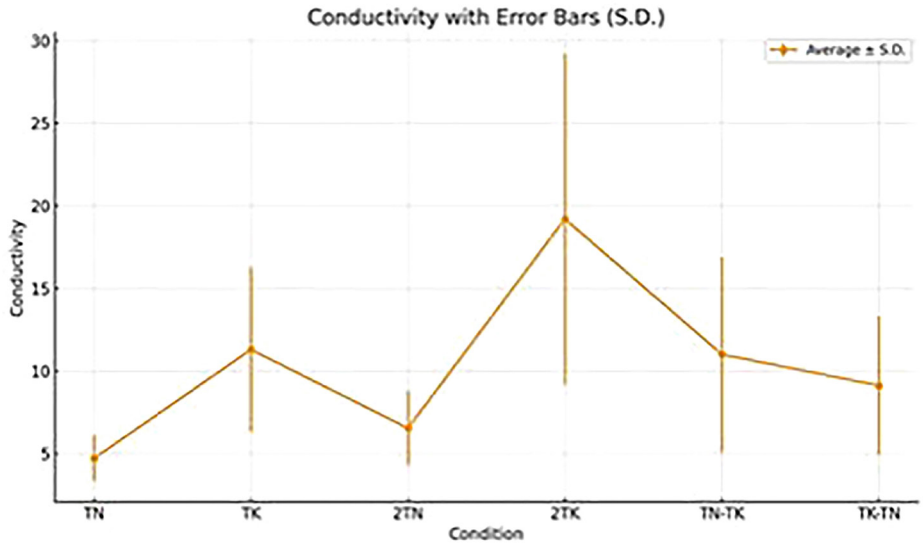

(b) Conductivity with Error Bars

Figure 13: Conductivity for due thickness.

Hence, the differences between the experimental and theoretical values of EVA thermal conductivity are justified by the fact that the theoretical values were obtained from virgin EVA, while the blankets tested here contain additives necessary for the production of soles. It can also be inferred that there is an influence of errors arising from the methods, such as the assumption of negligible convection, the time taken to soak the blanket in heat which was not sufficient, the method of fixing the blankets to the resistance in which some parts were more influenced by the pressure exerted by the adhesive tapes at the application site, among others.

In order to illustrate the results, the following Figure was constructed, Figure 13.

Figure 13 (a) was created to show the relationship between the conductivities and thicknesses of each blanket configuration. As the conductivity values of the blankets are much greater than their thickness, the log graph was chosen to be able to clearly visualize the illustrated values. The data Figure 13 (b) show that the cylindrical wall has a higher thermal efficiency than the flat wall under all test conditions. For example, under TN conditions, the cylindrical wall has an efficiency of 53.40%, while the flat wall has an efficiency of 31.62%. In the TK-TN case, the cylindrical wall has an efficiency of 79.40%, while the flat wall has only 64.50%, and this trend continues to the present. The efficiency of the two walls increases from simple heating conditions to more complex heating conditions, indicating that hybrid or combined heating configurations can improve heat transfer. The standard deviation is low, generally 3% to 5%, indicating that the measurement results are good and reliable. It is worth noting that the RSD value of the cylindrical wall is slightly lower, indicating a more stable or repeatable performance. Overall, the cylindrical wall provides the best and most reliable thermal efficiency, so when high and stable thermal efficiency is required, the flat wall has a lower efficiency, but is still stable.

In this Figure 13(a) it was possible to observe the variations in the conductivity of the material for each thickness, reaching the relationship that the minimum thickness of 3.3 mm (TNB) offered the lowest thermal conductivity of 0.66 $W/m°C$. The relatively high conductivity of TKBs may be due to the presence of pores with larger diameters when compared to those of 2TNB, which pass through the entire material. In this way, there is a direct transfer of heat through these pores through the TKBs, which does not happen in the 2TNB because the pores are smaller and retain the heat, a characteristic of a good insulator.

5.4. Analysis of compliance of methods with standards

ASTM standards do not impose any limitations on the design of new devices to be developed, as long as they meet certain requirements for their manufacture and all the methods already described by them.

Neither of the two proposed experimental methods were calibrated. For calibration, tests must be carried out with at least two standard insulation materials, such as glass or fiberglass, with known thermal properties, comparing the values found in the tests with those already known, thus determining a correction factor, thus ensuring the validation of the data obtained by the experiment.

According to ASTM C177 standard in item 7.1.2, it is recommended that the blankets be cut in such a way as to cover the entire surface of the hot source, thus minimizing loss at the edges. In the flat wall experiment, the blankets were cut into inadequate sizes because they were cut to dimensions of 210 mm × 210 mm for fixing to the 1020 steel hot plate with dimensions of 300 mm × 300 mm × 12.7 mm.

In the cylindrical wall experiment, the blankets were cut in such a way that it was possible to form a cylindrical shell and ensure full coverage of the entire surface area of the resistance, thus complying with the standard and ensuring less heat loss through convection.

Errors in the variation of ΔT can be caused by calibration and measurement errors, but also by the thermocouple itself. To avoid these errors, item 6.8.2.2 of ASTM C177 was followed. Small grooves were made on the surfaces of the samples and then thermocouples were fixed inside these grooves.

According to ASTM C 177, in item 7.2, which deals with sample preparation, it is recommended to condition the surfaces of the samples to ensure that they are parallel to each other, and the samples have uniform thermal contact.

According to ASTM C 177, in item 7.2, which deals with sample preparation, it is recommended to condition the surfaces of the samples to ensure that they are parallel to each other, and that the samples have uniform thermal contact with the heating and cooling plates.

In principle, a blowtorch would be used to heat the plate, which would generate uneven distribution of heat on the plate. Therefore, the assembly of the apparatus with a resistance proved to be closer to the standard, because this assembly provided a uniform temperature distribution.

5. CONCLUSION

The purpose of this study was to analyze and compare two methods to assess their adherence to established standards, thereby validating the data obtained and identifying potential improvements in the processes. The results indicated that the cylindrical wall experiment method incurred the lowest cost, amounting to ($0.042, which was significantly lower—by a factor of 29—compared to the cylindrical wall method, which cost ($1.25. Furthermore, the flat propagation method demonstrated conditions closer to real-life scenarios, as it allowed sufficient time for the blanket to absorb heat and reach equilibrium in the transfer rate at the end of each test.

In terms of thermal conductivity, the lowest value, indicating the highest attenuation, was observed for the TNB material (0.66 W/m°C), while the highest conductivity, representing the lowest attenuation, was recorded for the configuration with two TKBs (42.4 W/m°C). Both methods exhibited commonalities with current standards, with the primary requirement being the calibration of the device and the execution of tests using standard insulation materials with already determined properties.

Overall, based on the findings, the tested materials demonstrated potential for application as thermal insulators, exhibiting satisfactory attenuation levels.

7. ACKNOWLEDGMENTS

The authors express gratitude to their university, laboratory for providing necessary facilities, datasets, and resource access..

8. BIBLIOGRAPHY

[1] KIM, K.W., PARK, K.T., ATES, F., *et al.*, "Effect of pretreated biomass fly ash on the mechanical properties and durability of cement mortar", *Case Studies in Construction Materials*, v. 18, pp. e01754, 2023. doi: http://doi.org/10.1016/j.cscm.2022.e01754.

[2] KUSUMA, R.T., HIREMATH, R.B., RAJESH, P., *et al.*, "Sustainable transition towards biomass-based cement industry: a review", *Renewable & Sustainable Energy Reviews*, v. 163, pp. 112503, 2022. doi: http://doi.org/10.1016/j.rser.2022.112503.

[3] MOHAMAED, A., KMUDULI, K., "Utilization of biomass fly ash in cementitious application", *Journal of Physics: Conference Series*, v. 2129, n. 1, pp. 012005, 2021. doi: http://doi.org/10.1088/1742-6596/2129/1/012005.

[4] KOURDOURLI, F., ESTEL, L., TAOUK, B., *et al.*, "Modeling of hydrogen production from biomass bio-digestion under Aspen Plus", *Computers & Chemical Engineering*, v. 175, pp. 108273, 2023. doi: http://doi.org/10.1016/j.compchemeng.2023.108273.

[5] KASINATH, A., FUDALA-KSIAZEK, S., SZOPINSKA, M., *et al.*, "Biomass in biogas production: Pretreatment and codigestion", *Renewable & Sustainable Energy Reviews*, v. 150, pp. 111509, 2021. doi: http://doi.org/10.1016/j.rser.2021.111509.

[6] KONG, X., WEI, Z., XIA, S., *et al.*, "The characterizations of nanofluid type urea formaldehyde resins", *International Journal of Adhesion and Adhesives*, v. 126, pp. 103451, 2023. doi: http://doi.org/10.1016/j.ijadhadh.2023.103451.

[7] YE, H., ASANTE, B., SCHMIDT, G., *et al.*, "Eco-friendly geopolymer-wood building materials: Interactions between geopolymer and wood cell wall", *Journal of Cleaner Production*, v. 420, pp. 138381, 2023. doi: http://doi.org/10.1016/j.jclepro.2023.138381.

[8] BÖRCSÖK, Z., PÁSZTORY, Z., "The role of lignin in woodworking processes using elevated temperatures: an abbreviated literature survey", *European Journal of Wood and Wood Products*, v. 79, n. 3, pp. 511–526, 2021. doi: http://doi.org/10.1007/s00107-020-01637-3.

[9] KALAMI, S., CHEN, N., BORAZJANI, H., *et al.*, "Comparative analysis of different lignins as phenol replacement in phenolic adhesive formulations", *Industrial Crops and Products*, v. 125, pp. 520–528, 2018. doi: http://doi.org/10.1016/j.indcrop.2018.09.037.

[10] ELSHEIKH, A.H., PANCHAL, H., SHANMUGAN, S., *et al.*, "Recent progresses in wood-plastic composites: Pre-processing treatments, manufacturing techniques, recyclability and eco-friendly assessment", *Cleaner Engineering and Technology*, v. 8, pp. 100450, 2022. doi: http://doi.org/10.1016/j.clet.2022.100450.

[11] LERMAN, P., SCHEEPERS, G., "Determination of a mass-transfer coefficient for wood drying by means of thermography", *Wood Material Science & Engineering*, v. 18, n. 6, pp. 2104–2111, 2023. doi: http://doi.org/10.1080/17480272.2023.2243473.

[12] MISHRA, K., SIWAL, S.S., NAYAKA, S.C., *et al.*, "Waste-to-chemicals: green solutions for bioeconomy markets", *The Science of the Total Environment*, v. 887, pp. 164006, 2023. doi: http://doi.org/10.1016/j.scitotenv.2023.164006. PubMed PMID: 37172858.

[13] FAVIER, L., SIMION, A.I., HLIHOR, R.M., *et al.*, "Intensification of the photodegradation efficiency of an emergent water pollutant through process conditions optimization by means of response surface methodology", *Journal of Environmental Management*, v. 328, pp. 116928, 2023. doi: http://doi.org/10.1016/j.jenvman.2022.116928. PubMed PMID: 36521225.

[14] NÄGELE, H., PFITZER, J., NÄGELE, E., *et al.*, "Arboform: a thermoplastic, processable material from lignin and natural fibers", In: Hu, T.Q. (ed), Chemical Modification, Properties and Usage of Lignin, Cham, Switzerland, Springer, pp. 101–117, 2002. doi: http://doi.org/10.1007/978-1-4615-0643-0_6.

[15] CONSTANTINO, R.C., COELHO, L.B., PIVA, J.H., *et al.*, "Analysis of bond strength of adhesive mortars with different percentages of EVA exposed to hygrothermal cycles", *Matéria*, v. 27, n. 3, 2022. doi: http://doi.org/10.1590/1517-7076-RMAT-2022-0092.

9. DATA AVAILABILITY

The entire dataset supporting the results of this study was published in the article itself